



HAL
open science

Porous nickel and cobalt hexanuclear ring-like clusters built from two different kind of calixarene ligands – new molecular traps for small volatile molecules

Mariia Kniazeva, Alexander Ovsyannikov, Beata Nowicka, Nathalie Kyritsakas, Aida Samigullina, Aidar Gubaidullin, Daut Islamov, Pavel Dorovatovskii, Elena Popova, Sofiya Kleshnina, et al.

► To cite this version:

Mariia Kniazeva, Alexander Ovsyannikov, Beata Nowicka, Nathalie Kyritsakas, Aida Samigullina, et al.. Porous nickel and cobalt hexanuclear ring-like clusters built from two different kind of calixarene ligands – new molecular traps for small volatile molecules. *CrystEngComm*, 2022, 24 (2), pp.330-340. 10.1039/d1ce01361k . hal-03780239

HAL Id: hal-03780239

<https://cnrs.hal.science/hal-03780239>

Submitted on 19 Sep 2022

HAL is a multi-disciplinary open access archive for the deposit and dissemination of scientific research documents, whether they are published or not. The documents may come from teaching and research institutions in France or abroad, or from public or private research centers.

L'archive ouverte pluridisciplinaire **HAL**, est destinée au dépôt et à la diffusion de documents scientifiques de niveau recherche, publiés ou non, émanant des établissements d'enseignement et de recherche français ou étrangers, des laboratoires publics ou privés.

Porous nickel and cobalt hexanuclear ring-like clusters built from two different kind of calixarene ligands - new molecular traps for small volatile molecules

Received 00th January 20xx,
Accepted 00th January 20xx

DOI: 10.1039/x0xx00000x

Mariia V. Kniazeva,^a Alexander S. Ovsyannikov,^{a*} Beata Nowicka,^b Nathalie Kyritsakas,^c Aida I. Samigullina,^a Aidar T. Gubaidullin,^a Daut R. Islamov,^d Pavel V. Dorovatovskii,^e Elena V. Popova,^a Sofiya R. Kleshnina,^a Svetlana E. Solovieva,^b Igor S. Antipin,^b Sylvie Ferlay^{c*}

Two new isomorphous ring-like hexanuclear symmetrical coordination species ((**2-2H**)₂**3**)₂M₆, M = Co, Ni) presenting a hollow cyclic structure were successfully designed through the molecular recognition between the *in situ* generated sulfonylcalix[4]arene (**3**) supported trinuclear clusters and flexible macrocyclic linkers based on the low rim appended calix[4]arene diacid derivative (**2-4H**) demonstrating a pincer-like shape. The obtained coordination compounds have been characterized from a structural point of view in the crystalline phase revealing the formation of internal hydrophobic voids, passing through the hexameric units, and external voids, resulting from the packing of the complexes in the lattice. A slight structural transformation was evidenced upon air-drying, leading to the closure of external voids caused by the solvent release and also the solvent mobility within the network. The ability of obtained desolvated solid-state hexanuclear species to uptake small volatile molecules like H₂O, CH₃C(O)CH₃, MeOH and EtOH has been investigated by dynamic vapor sorption (DVS) showing their high affinity towards more polarizable molecules.

Introduction

Porous molecular coordination compounds, such as metal-organic frameworks¹ and coordination cages or polyhedra,^{2,3} are the subject of a great interest, especially due to their intriguing architectures and unique physical and chemical properties which can be tuned by a judicious choice and selection of metal ions or metallic clusters showing several coordination geometries as well as organic ligands presenting attractive shapes.⁴ Molecular structures displaying intrinsic porosity in the crystalline phase may find applications in molecular separation/storage, sensing^{5,6} and transport materials, for example.^{7,8} As known, the void spaces within the crystal lattice of the coordination compounds (host network) are commonly filled by solvent molecules (guest molecules) : the interactions are generally ensured by non-covalent interactions between both partners. As usual, after solvent removing, the generated pores are activated and available for adsorption, eventually selective, for new guests. Thus, achieving the formation of crystalline phase with controlled porosity is one motivation when designing porous materials and it is still

quite challenging.⁹ In this aspect, over a past decade, a huge number of ligands were involved in the building of porous crystalline materials, exhibiting specific adsorption properties. Among them, macrocyclic compounds¹⁰ like calix[4]arenes^{11,12} appear very attractive, owing to the presence of the hydrophobic cavity composed of four aromatic rings adopting different conformations, which, therefore, can be used for accommodation of different organic molecules or gases.¹³ Calixarenes belong to a family of versatile organic ligands, which synthesis can be achieved in only one stage. They display a great thermal stability, can be practically indefinitely chemically modified by adding different functional groups both at their lower and/or upper rims. When functionalized or not, they are able to bind metallic cations, forming thus coordination compounds of various dimensionalities (0D-3D), exhibiting attractive physical properties.¹⁴ One of particular features of these macrocycles, especially *p*-*tert*-butylcalix[4]arene ((**1-4H**), figure 1) and *p*-*tert*-butylthiacalix[4]arene (sulphurated analogue of **1-4H**),¹⁵ is their fantastic ability to form high nuclearity coordination compounds.^{16,17,18,19} Their analogue, tetrasulfonylcalix[4]arene (**3-4H**),²⁰ shown in figure 1, also represents a very suitable polydentate ligand offering four phenolate groups together with four sulfonyl moieties as coordinating sites, to form coordination clusters.^{21,22} Metallamacrocyclic, capsules, (super)containers^{23,24} and cages,^{25,26,27} all these sophisticated finite coordination species have been obtained both with *p*-*tert*-butylthiacalix[4]arene and tetrasulfonylcalix[4]arene (**3-4H**), sometimes combined with ancillary ligands, and displaying up to 40²⁸ or 48²⁹ metallic atoms within the clusters. Giant wheels with tuneable number of metallic atoms have been also reported.³⁰ It was found that these discrete supramolecular architectures can exhibit different fascinating functions such as: sensing,³¹ protons reservoir,³² catalysis^{33,34} or enantioselective catalysis,³⁵

^a Arbutov Institute of Organic and Physical Chemistry, FRC Kazan Scientific Center, Russian Academy of Sciences, Arbuzova 8, Kazan, 420088, RUSSIAN FEDERATION

^b Laboratory for structural analysis of biomacromolecules, Kazan Scientific Center of Russian Academy of Sciences, Lobachevskogo 2 str, Kazan 420008, RUSSIAN FEDERATION

^c Kazan Federal University, Kremlevskaya 18, Kazan 420008, RUSSIAN FEDERATION

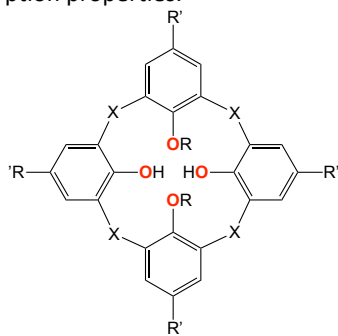
^d National Research Centre "Kurchatov Institute", Acad. Kurchatov 1 Sq., 123182 Moscow, RUSSIAN FEDERATION

^e Université de Strasbourg, CNRS, CMC UMR 7140, F-67000 Strasbourg, FRANCE

† Footnotes relating to the title and/or authors should appear here.

Electronic Supplementary Information (ESI) available: For (**2-2H**)₂**3**)₂M₆ (M = Co or Ni) representation of the supramolecular interactions and visualizations of the channels, TGA traces, XRPD traces, N₂ adsorption properties, solvent adsorption properties, SEM images and cycling of the water absorption. See DOI: 10.1039/x0xx00000x

hydrogen evolution activity³⁶ and redox properties tuning thus the gas adsorption properties.³⁷



- 1-4H: X = CH₂; R = H; R' = *t*-But
 2-4H: X = CH₂; R = CH₂COOH; R' = *t*-But
 3-4H: X = SO₂; R = H; R' = *t*-But
 4-4H: X = CH₂; R = C₃H₆COOH; R' = *t*-But

Figure 1: The different macrocycles belonging to the calix[4]arene family used for the building of coordination compounds

As already stated, calix[4]arene moieties are inherently well suited for trapping different guest molecules in the solid state, that has been well documented nearly 2 decades ago. One can notice the pioneering work performed by Atwood *et al*, where *p*-*tert*-butylcalix[4]arene, in nonporous solids, undergo significant positional and/or orientational rearrangement to facilitate guest uptake and release.³⁸ In general this family of compounds present low Surface areas values. In addition, such solid state materials revealed to be efficient for gas separation, towards H₂, for example³⁹ or other gaseous molecules (O₂, N₂, CH₄, CO₂, C₂H₄).^{40,41} These macrocyclic species (calix[4]arenes or tetrasulfonylcalix[4]arene) when involved in capsules⁴² or forming diamond-like crystalline structures,⁴³ are also able to behave as adsorbent for unsaturated hydrocarbons, polarizable inert gases, and also for carbon dioxide.

Concerning solvent vapors adsorption of calixarene derivatives in the solid state, a number of studies has been also reported. It was shown that conventional calix[4]arene based compounds can form clathrates when interacting through the gaseous phase with a great number of organic volatile molecules such as toluene, acetonitrile, propionitrile, chloroform, tetrachloromethane, showing a remarkable guest binding properties.^{44,45} When functionalized with four methylenecarboxylic groups, *p*-*tert*-butylthiacalix[4]arene enhances its receptor capacity and affinity towards water and aliphatic alcohols (methanol and ethanol)⁴⁶ and carboxylic acids.⁴⁷

For the extended coordination networks based on calixarenes, one can note a 2D nanotube, built from *p*-*tert*-butylthiacalix[4]arene, that represents a promising material for separating C₂H₆ and C₃H₈ from CH₄⁴⁸ and also a 3D coordination network based on modified *p*-*tert*-butylthiacalix[4]arene exhibiting substantial CO₂ uptake.⁴⁹ Another interesting example was coming from a solid obtained from a mixture of Calix[4]arene derivatives and polyoxometalate, displaying a porous structure, and unique guest binding properties.⁵⁰ The

porous properties of coordination complexes based on calixarenes have been scarcely reported.^{28,51}

We intend to investigate the sorption properties of new coordination compounds based on calix[4]arene. Recently, we developed a novel strategy for the formation of coordination species with controlled nuclearity: the combination of the macrocyclic calix[4]arene based ligands (**3-4H**) and a pincer-like (**4-4H**) with metallic salts (M = Zn, Co and Ni) leads to the formation of non-symmetrical trinuclear capsules.⁵² This was also recently confirmed using another pincer like analogue, presenting benzoate ligand leading also to a trinuclear Zn(II) coordination compound.⁵³

In this work, using a calixarene based ligand (**(2-4H)**, figure 1) presenting a shorter spacer than (**4-4H**), two isomorphous polynuclear complexes have been obtained. But in contrast to what have been already observed using this approach, hexanuclear ring-like coordination species have been obtained and structurally characterized using X-ray diffraction on single crystals. Their stability has been studied. The sorption abilities of these finite coordination compounds towards vapor small organic guests and water molecules have been investigated using DVS.

Results and discussion

Synthesis of the coordination compounds

In the present paper, new coordination compounds have been synthesized using solvothermal conditions (microwave heating), for a multicomponent system composed of (**2-4H**), (**3-4H**) and nitrate salts M(NO₃)₂ (M=Co, Ni) in a DMF/MeOH mixture, followed by a slow evaporation of the solvents at room temperature under aerobic conditions (see experimental section). Suitable crystals for X-Ray diffraction have been reproducibly obtained. The structure is described below.

Structural characterization of (**(2-2H)₂3₂M₆**) by single crystal X-ray diffraction

The X-ray diffraction analysis revealed the formation of a symmetric hexanuclear complex presenting the following formula (**(2-2H)₂3₂(M₃(OH)₂)₂(DMF)₂ • x DMF**) (**(2-2H)₂3₂M₆**, M = Co, Ni, x = 12 and 4, respectively). Squeeze command⁵⁴ was applied for the refinement of (**(2-2H)₂3₂Co₆**), and for (**(2-2H)₂3₂Ni₆**) an analogous command have been used in the *Olex2* software.⁵⁵ 10 uncoordinated DMF molecules were refined in the unit cell for (**(2-2H)₂3₂Co₆**), whereas 4 molecules have been successfully refined for (**(2-2H)₂3₂Ni₆**). The compounds crystallize in the triclinic system, space group *P* $\bar{1}$, as shown in the crystallographic table 1. Both compounds are isomorphous and differs only by the quantities of refined solvent molecules.

Since both obtained complexes are isomorphous and isometric, only the description of the crystal structure will be given only for (**(2-2H)₂3₂Co₆**).

Crystals of (**(2-2H)₂3₂Co₆**) are composed of two di- deprotonated ligands (**(2-2H)²⁻** (confirmed by the C-O distances, see table 2), two tetra- deprotonated ligands **3⁴⁻**, six Co²⁺ cations, one coordinated water molecule, one μ_3 -coordinated water

molecule, two coordinated DMF molecules and 10 lattice DMF molecules located in the unit cell. In this compound, both $(2-2H)^{2-}$ and 3^4- are cone shaped which is in accordance with the previously reported data for their related coordination compounds.^{52,53} Neutral hexanuclear ring-shaped clusters result from the bridging of trinuclear $[3(M_3DMF(OH_2)_2)]^{2+}$ entities by $(2-2H)^{2-}$ units and present inversion symmetry centre located between the trimetallic nodes, leading to the formation of internal spherical cavity with a diameter of *ca* 8.2 Å, an external diameter of *ca* 26 Å. The obtained compound displays a disc shape as shown in figure 2 a-b, with a thickness of *ca* 10 Å, and finally a ring like shape with a pore of 8.2 Å, in the middle of the disc.

The environment around each of the three crystallographically independent Co^{2+} cations is a deformed octahedron, as shown by the bonds and distance (see Table 2), with 6 O atoms derived from the carboxylic moieties, sulfonate groups and DMF, as shown in figure 2c. One of the Co^{2+} cations is also bearing a free water molecule. Metallic triangles are formed within the $[3(M_3DMF(OH_2)_2)]^{2+}$ entities, involving two short (3.0102(36) and 3.0233(21) Å) and one long (3.8144(30) Å) Co-Co distances (see Table 2), a μ_3 -coordinated water molecule, as already observed for trinuclear based compounds,^{52,53} is present in the middle of the non-isosceles triangle, with Co-O distances in the 2.044(3)-2.100(3) Å range.

	$(2-2H)_23_2Ni_6$	$(2-2H)_23_2Co_6$
M-O	2.011(4)	2.014(4)
	2.015(4)	2.042(3)
	2.027(4)	2.051(3)
	2.033(4)	2.055(3)
	2.036(4)	2.065(4)
	2.041(5)	2.071(3)
	2.043(4)	2.081(3)
	2.064(5)	2.094(3)
	2.065(4)	2.108(3)
	2.073(4)	2.111(4)
	2.074(4)	2.111(3)
	2.076(5)	2.112(3)
2.078(5)	2.120(3)	
M- O_{DMF}	2.040(6)	2.104(5)
M- O_{H_2O}	2.053(5)	2.074(4)
M- $\mu_3O_{H_2O}$	2.036(4)	2.044(3)
	2.038(4)	2.071(3)
	2.046(4)	2.100(3)
M-M (trinuclear)	2.9728(12)	3.0102(36)
	2.9673(15)	3.0233(21)
	3.7860(12)	3.8144(30)
C-O (carboxylate) for $(2-2H)^{2-}$	1.248(8) + 1.253(7)	1.230(6) + 1.246(6)
	1.260(7) + 1.260(7)	1.248(6) + 1.251(6)

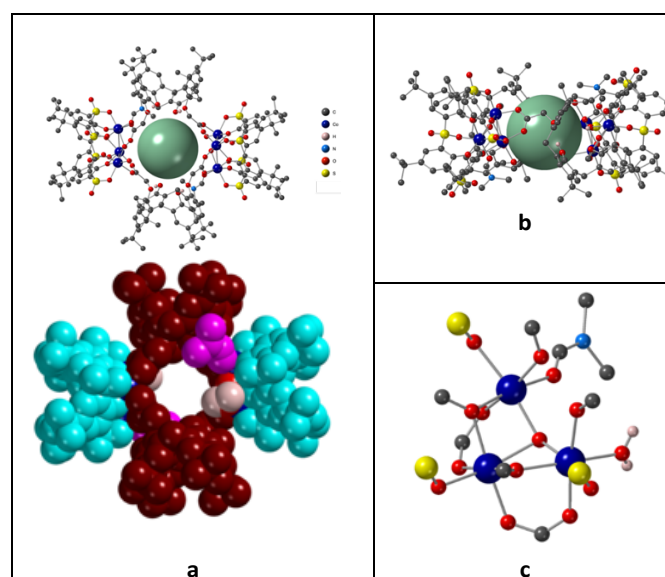
Table 2. Characteristic bond distances for $(2-2H)_23_2Ni_6$ and $(2-2H)_23_2Co_6$ determined using X-Ray diffraction on single crystals.

The porous character of $(2-2H)_23_2Co_6$ is evidenced by the formation of two types of nanosized tubular channels resulting from the parallel stacking of the coordination compounds along the *a* axis upon the crystal packing (figure 2d and figure S2, ESI). The channels belonging to the first type, with a diameter of *ca*

8.2 Å (internal channels in green in figure 2d) pass through the inner cavity of the hexanuclear units and DMF lattice molecules occupy these channels, whereas the second type of channels (external channels in pale pink in figure 2d) are placed in the interstices between the stacked complexes with a diameter of *ca* 7.6 Å. There are narrow interconnections between the two types of channels (figure S2). In addition, the crystal of $(2-2H)_23_2Co_6$ demonstrates the formation of supramolecular capsule-like fragments obtained by the “face-to-face” orientation of hydrophobic hexanuclear cavities, as depicted in Figure 2d.

One of the refined lattice DMF molecules (N5) forms a hydrogen bond through the carbonyl oxygen to coordinated water ($O22$) with $d_{O-O} = 2.65$ Å. Moreover, some non-classical hydrogen bonding between accommodated DMF molecules and tert-butyl groups of macrocycles $(2-2H)^{2-}$ and 3^4- are observed with the $d_{O-C} = 3.51-3.58$ Å.

The refined 10 DMF lattice molecules also form C-H- π interactions with calixarene aromatic rings (Figure S1, ESI), with the exception of two DMF molecules (N6) located inside the internal channels, as shown in figure 2d. Four DMF molecules (N3 and N7) are trapped in the external channels $(2-2H)^{2-}$ and 3^4- by multiple interactions between methyl group and aromatic rings with the C-ring centroid distances in the range of 3.54-3.70 Å. The six DMF molecules located between the calixarenes (N2, N4, and N5) also show C-H- π interactions through both methyl and carbonyl groups.



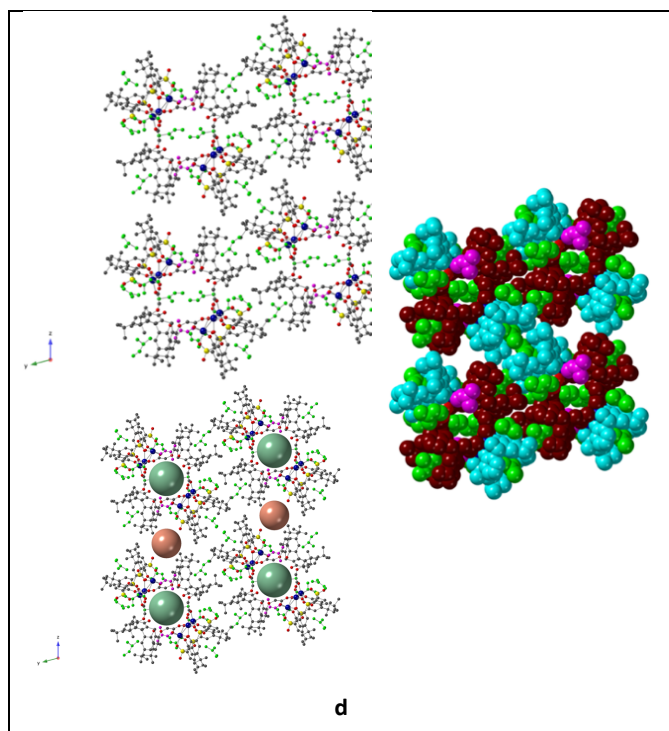


Figure 2. The structure of $(2-2H)_2\mathbf{3}_2Co_6$ established by X-Ray diffraction on single crystals: a) the hexanuclear ring shaped coordination compound formed by $(2-2H)^{2+}$ and 3^{4-} presenting a spherical cavity in the middle, top view (molecular and space-filling representation), b) side view, c) the coordination environment of the metal ions within the trinuclear cluster core and d) crystal packing (molecular and space filling representation) showing the formation of tubular channels (“Internal” = green, “External” = pale pink) along the a axis (the coordinated and lattice DMF molecules are represented in pink and green, respectively) and supramolecular cages formed by face to face orientated hydrophobic calixarene cavities (blue color). H atoms are omitted for clarity. For bond distances and angles see the text and Table 2.

Due to the presence of a large number of solvents in the crystal (squeezed in the refinement), the stability of the crystalline powder was firstly studied using PXRD measurements.

Structural behavior of the polycrystalline powder

The purity of $(2-2H)_2\mathbf{3}_2Co_6$ and $(2-2H)_2\mathbf{3}_2Ni_6$ powdered samples was investigated by PXRD (see Figure S3, ESI). The measurements reveal that no other crystalline phase was observed in the powdered samples.

The time dependence behaviour of the microcrystalline powder has been further explored (figure 3) for $(2-2H)_2\mathbf{3}_2Co_6$: when exposed to the air more than one hour after separation from the mother liquor, the freshly prepared powdered compound displays some structural modifications associated with the release of some of the lattice solvent molecules, which probably include DMF, as well as MeOH and H_2O that have not been refined during structure refinement. Unfortunately, the poor resolution of the PXRD patterns didn't allow us to precisely refine the unit cell parameters after the irreversible transformation.

As shown by the slight shifts and broadening of the peaks on the XRPD pattern, during the exposure to the air, the transformation doesn't affect the structure of the hexanuclear units but their environment.

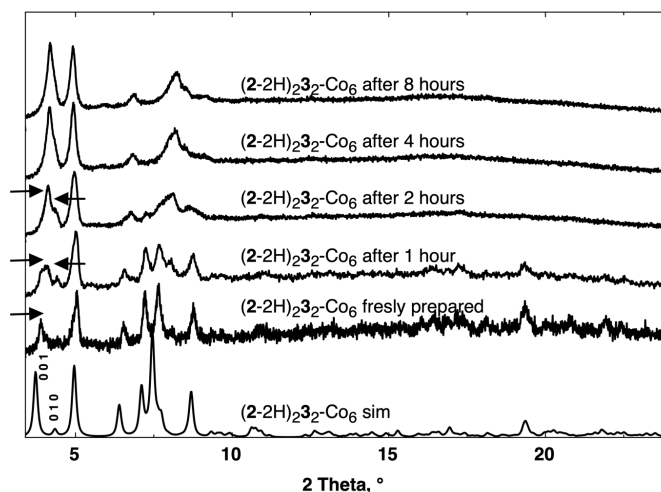


Figure 3. For $(2-2H)_2\mathbf{3}_2Co_6$, the time-resolved PXRD diagrams of the powdered sample in comparison with the simulated one showing a desolvation of the freshly synthesized compound when exposed to the air.

As already mentioned, the crystal structure of $(2-2H)_2\mathbf{3}_2Co_6$ contains two types of 1D void channels: “External” and “Internal” voids (see figure 2d also figure S2, ESI). “External” voids can be considered as quite flexible due to the possible loss and moving of the solvent molecules. The distances between the centres of the “Internal” voids along the Ob and Oc crystallographic axis of $(2-2H)_2\mathbf{3}_2Co_6$ can be described by the values of the cell parameters b (21.556 (4) Å and 21.7263(7) Å for M=Ni and Co, respectively) and c (24.370 (5) Å and 24.4931(9) Å for M=Ni and Co, respectively) as shown in figure 4. After a long exposure to the air, the formation of a wide peak at $2\theta = 4.48^\circ$ (figure 4) can be assigned to the shifting of two symmetry planes (010) and (001) within the crystalline phase due to closing of “External” voids disposed between the complex molecules. One of possible mechanism of voids collapsing is proposed in figure 4. The final structure is stable though the contribution of H bonds, C-H- π , van der Waals and interdigitation of chains, involving all the components present in the lattice.

The same observation was performed for of $(2-2H)_2\mathbf{3}_2Ni_6$, as shown by the XRPD diagrams (figure S3, ESI).

This proposed mechanism appears to be irreversible: after soaking the polycrystalline powder or crystals in a 1/1 H_2O/DMF solution during 1 hour, they display the same PXRD pattern as displayed after 4 hours when exposed to the air.

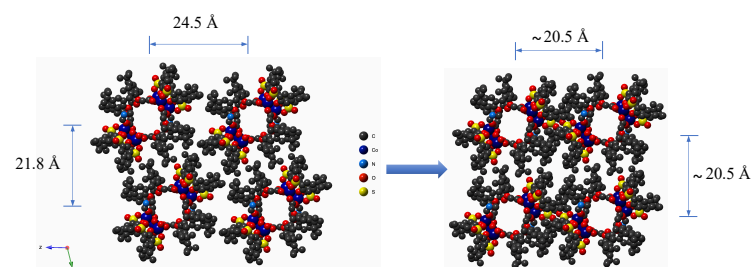


Figure 4. The proposed mechanism of “external” voids closing upon exposure to the air for $(2-2H)_2\mathbf{3}_2Co_6$. For clarity reasons, all refined lattice DMF solvent molecules have not been represented.

Thermal behavior of the polycrystalline powder

The TGA measurements for microcrystalline powder of $(2-2H)_2\mathbf{3}_2Co_6$ and $(2-2H)_2\mathbf{3}_2Ni_6$ (Figure S4, ESI) show that the mass loss begins at ambient conditions and there is no plateau at the start of the experimental curves. This is consistent with the presence of crystallization solvents in the crystal and changes in PXRD described above during desolvation process. The $(2-2H)_2\mathbf{3}_2Ni_6$ compound shows a distinct desolvation step with T_{max} at 115°C, which is completed at about 200 °C. In the case of $(2-2H)_2\mathbf{3}_2Co_6$, the initial mass loss step is prolonged to 280°C and it is clearly composed of overlapping processes evidenced by the presence of inflection points in TG and indistinct minima in DTG. For both compounds the decrease in mass in this step is about 17 %. The decrease in mass of 17 % is slightly lower than the release of 12 DMF molecules (10 lattice and 2 coordinated) and 2 coordinated H₂O that have been refined using XRD, for $(2-2H)_2\mathbf{3}_2Co_6$. The presence of other unrefined molecules cannot be excluded and cannot be further quantified. The shape of the TG curves of Co and Ni based compounds suggest that in the first step both lattice (10 DMF) and coordinated (2 H₂O and 2 DMF) solvent molecules are released.

N₂ sorption properties of $(2-2H)_2\mathbf{3}_2M_6$

The N₂ sorption properties of both coordination compounds have been first investigated. $(2-2H)_2\mathbf{3}_2Co_6$ and $(2-2H)_2\mathbf{3}_2Ni_6$ exhibit a BET surface area of 77.6 and 132.5 m²/g respectively (see isotherms at 77K, figure S6, ESI). This is a very low value, but in accordance with what has been frequently observed for other calixarene coordination compounds. Though they are isostructural, both compounds display a slightly different sorption behaviour, which can mainly be attributed to the different grain morphology of both polycrystalline samples, as attested by the recorded SEM images (figure S8, ESI).

Solvent sorption properties of $(2-2H)_2\mathbf{3}_2M_6$

The possibility of sorption of small solvent molecules, H₂O, MeOH, EtOH and CH₃C(O)CH₃, into the porous structure of $(2-2H)_2\mathbf{3}_2Ni_6$ and $(2-2H)_2\mathbf{3}_2Co_6$ was investigated by the gravimetric dynamic vapor sorption (DVS) technique.

Firstly, the activation of compounds was performed under a range of mild conditions: humid atmosphere and low temperature. The preliminary experiments at 25°C show very slow decrease in mass of the air-dried polycrystalline sample of $(2-2H)_2\mathbf{3}_2Co_6$ in the flow of dry N₂. When the humidity is increased stepwise, in each step the sharp initial increase in mass, caused by the intake of water, is followed by gradual, almost linear mass loss (see figure 5). This unusual behavior indicates that the removal of solvent DMF is assisted by water molecules. The mechanism of this humidity-assisted desolvation of DMF may be explained in terms of intermolecular interactions: the surface of the solvent-accessible cavities in the structure is mostly hydrophobic and water molecules penetrating into the channels may form hydrogen bonds, stronger than C-H- π interactions and may draw the DMF molecules sandwiched between or nestled inside calixarene

cavities, thus increasing their mobility. The complete desolvation of both compounds was achieved by exposure to 30% RH at 50°C for 12 h followed by dehydration at 0% RH to constant mass ($dm/dt < 0.002$ %/min). The decrease in mass from the air-dried form of ca. 12 % corresponds approximately to the removal of 10 lattice DMF molecules. It is consistent with the results of the elemental analysis for the air-dried forms, which show the presence of 12 DMF molecules, two of which are coordinated.

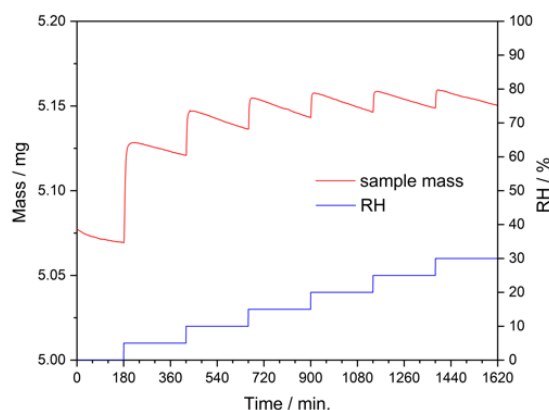


Figure 5. Mass change of $(2-2H)_2\mathbf{3}_2Co_6$ at 25°C with stepwise changes in RH illustrating the humidity-assisted DMF desolvation process.

After the desolvation has been completed, the powdered sample of $(2-2H)_2\mathbf{3}_2Ni_6$ exhibits a PXRD profile (Figure S5, ESI) very similar to the one observed for the air-dried $(2-2H)_2\mathbf{3}_2Co_6$ crystals (see figures S3 and 3), accounting for the fact that the compound doesn't present any significant structural changes upon desolvation.

The completely desolvated compounds $(2-2H)_2\mathbf{3}_2Co_6$ and $(2-2H)_2\mathbf{3}_2Ni_6$ were subjected to the dynamic vapor sorption studies under atmospheric pressure with changeable partial pressure of water or volatile organic solvents. The guest molecules, H₂O, CH₃C(O)CH₃, EtOH and MeOH, were chosen to fit the size of the internal channels in the structure.

The water sorption isotherm for $(2-2H)_2\mathbf{3}_2Co_6$ in the range of 0 to 98% RH (Figure 6) is characterized by slow gradual mass increase after the initial step of about 2 % with slightly higher increase at high humidity, most probably connected with surface effects. The sorption process is reversible with a very narrow reproducible hysteresis. The maximum mass change (ca. 7% in relation to the desolvated compound mass) corresponds to the intake of 15 H₂O molecules, which suggests that they fill only part of the solvent accessible void, which volume in the original structure exceeds 1600 Å³ (for non-air-dried compound).

The sorption of organic solvent vapors (CH₃C(O)CH₃, EtOH and MeOH) shows similar gradual characteristics, with slightly sharper initial step for CH₃C(O)CH₃. However, the desorption process requires lower partial pressure, which results in much wider hysteresis. Moreover, the maximum intake of guest molecules, despite their large size, is higher than in the case of

water and can be estimated at 17 molecules for $\text{CH}_3\text{C}(\text{O})\text{CH}_3$ and EtOH and 21 molecules for MeOH (see table 3). The difference in the sorption characteristics between water and organic solvent vapors indicates that larger molecules with lower polarity fill the voids more efficiently and are more effectively retained in the structure, probably due to the formation of C-H- π interactions between the CH_3 groups of organic solvents and calixarene aromatic rings, which enables better penetration of the guest molecules into the structure and their binding by the prevalent hydrophobic regions. Similar effects of the absorbed MeOH and EtOH filling only part of the void volume was observed for a Ni-based MOF structure.⁵⁶

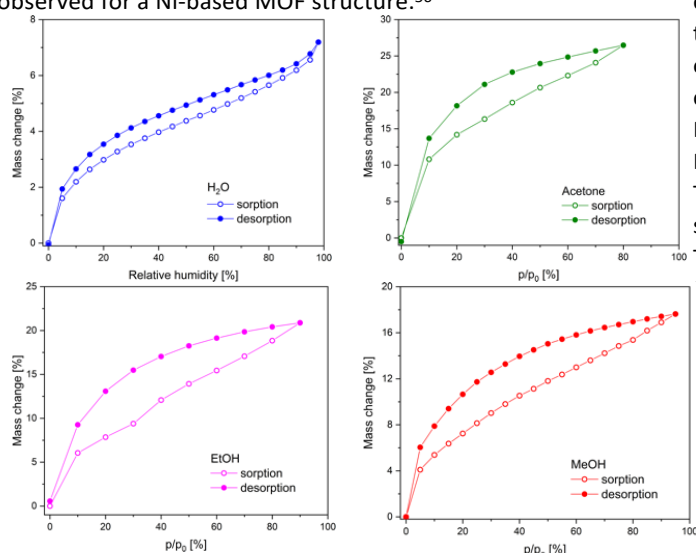


Figure 6. Sorption isotherms of H_2O , $\text{CH}_3\text{C}(\text{O})\text{CH}_3$, EtOH and MeOH for $(2-2\text{H})_2\mathbf{3}_2\text{Co}_6$ at 25°C.

The $(2-2\text{H})_2\mathbf{3}_2\text{Ni}_6$ compound shows similar sorption characteristics to its Co-based analogue, with reversible gradual intake of water and organic vapors (Figure S9, ESI). However, there are some differences between both compounds. The maximum water intake by $(2-2\text{H})_2\mathbf{3}_2\text{Ni}_6$ of 4.4% corresponds to about 9 H_2O , and is much lower than that observed for $(2-2\text{H})_2\mathbf{3}_2\text{Co}_6$. The amount of absorbed organic solvent molecules is comparable (17 EtOH) or slightly lower (16 MeOH, 13 $\text{CH}_3\text{C}(\text{O})\text{CH}_3$) than for the Co analogue (see table 3). Moreover, the sorption of organic solvent vapors shows indistinct steps, with higher mass increase at the partial pressure (p/p_0) of 5% and 25-30%. Together with gradual desorption over the whole p/p_0 range it results in a narrower and slightly irregular shape of the hysteresis.

	H_2O	$\text{CH}_3\text{C}(\text{O})\text{CH}_3$	MeOH	EtOH
$(2-2\text{H})_2\mathbf{3}_2\text{Ni}_6$	9	13	16	17
$(2-2\text{H})_2\mathbf{3}_2\text{Co}_6$	15	17	21	17

Table 3. Number maximal of solvent intake in $(2-2\text{H})_2\mathbf{3}_2\text{Ni}_6$ and $(2-2\text{H})_2\mathbf{3}_2\text{Co}_6$, evaluated by Dynamic Vapor Sorption studies

The differences in the sorption behavior between $(2-2\text{H})_2\mathbf{3}_2\text{Co}_6$ and $(2-2\text{H})_2\mathbf{3}_2\text{Ni}_6$ suggest that despite their “isostructurality”,

for both compounds, the air-drying and desolvation process, which causes closing of the external voids, results in some small structural differences, which probably affect subtle intermolecular interactions with guest molecules, even though they are not apparent in PXRD studies. This supposition is supported by the differences in morphology between the microcrystalline air-dried samples visible in SEM images (figure S8, ESI), where needle-like crystals can be observed for $(2-2\text{H})_2\mathbf{3}_2\text{Ni}_6$, while $(2-2\text{H})_2\mathbf{3}_2\text{Co}_6$ is characterized by irregularly-shaped particles.

For both compounds the sorption/desorption hysteresis are closed and reproducible in subsequent cycles, which indicates that the sorption processes are fully reversible. The reversibility of the water sorption was additionally studied by repeated cycles in which the samples were subsequently exposed to dry N_2 and maximum partial pressure of solvent vapors (98% for H_2O , 80% for $\text{CH}_3\text{C}(\text{O})\text{CH}_3$, 90% for EtOH), or 95% for MeOH). The representative results are shown for water sorption/desorption for $(2-2\text{H})_2\mathbf{3}_2\text{Co}_6$ in figure S8, ESI.

The shape of the sorption isotherms with larger initial intake followed by gradual mass increase with lack of pronounced sharp steps and uniform hysteresis is characteristic for rigid porous structures, where no structural changes in response to incoming guest molecules are observed. This assumption is supported by lack of changes in the PXRD pattern after water sorption (Figure S5, ESI). The intake of volatile solvents by $(2-2\text{H})_2\mathbf{3}_2\text{M}_6$ ($\text{M} = \text{Co}, \text{Ni}$) is significantly higher than that observed in DVS studies for non-porous structures.⁵⁷

Discussion

All performed physico-chemical studies are consistent with the fact, that the formed crystalline isomorphous compounds $(2-2\text{H})_2\mathbf{3}_2\text{M}_6$ ($\text{M} = \text{Ni}$ and Co) are based on the assembly, in the crystalline state, of ring like symmetrical hexanuclear coordination compound, glued by solvent molecules, DMF and probably H_2O and MeOH, leading to the formation of external and internal (center of the ring) channels. The localization of the lattice refined solvent molecules is ensured by weak intermolecular interactions (H-bonds and C-H- π interactions). It was found that the air-dried samples of $(2-2\text{H})_2\mathbf{3}_2\text{M}_6$ ($\text{M} = \text{Ni}$ and Co) undergo an irreversible structural transformation inducing a partial loss of crystallinity, and that is probably caused by the high mobility of the free DMF solvents within the structure, and shifting of crystallographic planes. In air dried microcrystalline compounds, the hexanuclear coordination compound remain unchanged, but the external channels are closed. The DMF solvent molecules are still weakly interacting with the complexes, but additional interdigitation between the complexes and van der Waals interactions ensure the cohesion of the crystal.

When the air-dried microcrystalline compounds are exposed to humidity and slightly increased temperature, they can be desolvated: lattice solvent molecules (among them 10 DMF) are released, suggesting a water assisted desolvation process. The ordering of the desolvated samples in the solid state remains unchanged, suggesting the stability of the air-dried

state of compounds, proving the possibility of solvents to move in or out the lattice whereas the hexanuclear species are found immobile after external voids closure has been performed. This suggestion was attested by PRXD experiments revealing the same patterns observed for air-dried and desolvated compounds. Such transformations undergoing in the crystalline phase of obtained supramolecular complexes can be depicted in the figure 7.

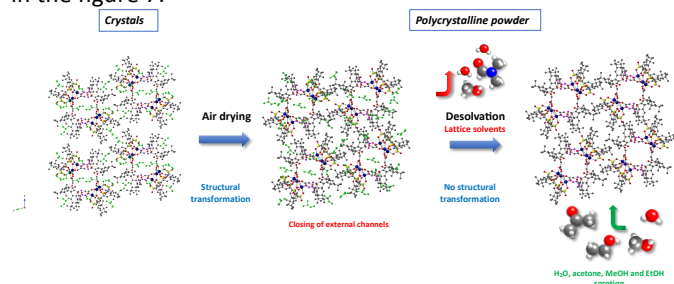


Figure 7. Air drying and desolvation process for $(2-2H)_23_2M_6$ ($M = Ni$ and Co) related to structural transformations. The coordinated and lattice DMF molecules are represented within the network in pink and green, respectively.

It was also shown, that crystalline powder of obtained ring like architectures present guest binding properties towards small solvent molecules: H_2O , $CH_3C(O)CH_3$, $MeOH$ and $EtOH$, due to enhanced stability of the pores ensured by the rigidity of the scaffold of supramolecular complexes. The abilities of these small molecules to be trapped into the large internal channels has been studied, evidencing a reversible process.

Experimental

Synthesis

General: All reagents and solvents were of analytical grade and purchased from commercial sources and were used without further purification. The synthesis of (2-4H) was adapted from an already reported procedure.⁵⁸ The synthesis of (3-4H) was achieved following the described procedure.²¹

(2-2H)₂3₂Co₆: Compounds (2-4H) (30 mg, 0.035 mmol), (3-4H) (27 mg, 0.035 mmol) together with $Co(NO_3)_2 \cdot 6H_2O$ (51 mg, 0.177 mmol) were dissolved in DMF/MeOH mixture (6,3 mL) and put into a Pyrex crystallization reactor equipped with a screw cap. Then, the solution was heated under MW irradiation conditions (100 W) and stirred for 3 hours. After cooling and filtration, the light rose single crystals suitable for X-ray diffraction analysis were obtained upon slow evaporation of the mother liquor at room temperature in 7 days under aerobic conditions. Total yield: 40 mg (50%). Formula: $C_{212}H_{294}N_{12}O_{56}S_8Co_6$, Anal. Calcd.: C, 56.37%; H, 6.56%; N, 3.72%; Found: C, 56.04 %; H, 6.63%; N, 3.95 %. IR (cm^{-1}): 3391, 2961, 2870, 1714, 1765, 1630, 1607, 1502, 1386, 1363, 1332, 1290, 1262, 1220, 1195, 1128, 1081, 904, 872, 839, 794, 750, 697, 669, 626, 562 (see figure S9, ESI).

(2-2H)₂3₂Ni₆: The same procedure was repeated starting from $Ni(NO_3)_2 \cdot 6H_2O$ and leading to light green single crystals suitable for X-ray diffraction analysis were obtained upon slow evaporation of the mother liquor at room temperature in 7 days under aerobic conditions. Total yield: 41 mg (51%). Formula: $C_{212}H_{294}N_{12}O_{56}S_8Ni_6$, Anal. Calcd.: C, 56.39%; H, 6.56 %; N, 3.72%; Found: C, 56.17%; H, 6.66%; N, 4.21%. IR (cm^{-1}): 3368, 2962, 2871, 1714, 1761, 1630, 1606, 1493, 1387, 1363, 1333, 1294, 1264, 1222, 1160, 1130, 1084, 1047, 907, 872, 801, 749, 702, 660, 627, 560 (see figure S9, ESI).

Characterization techniques

The IR spectra of the polycrystalline samples were recorded on a Bruker Tensor 27 spectrometer (Bruker Optic GmbH, Germany) in KBr pellets.

Elemental analysis was performed on a Vario Macro CHN Analyzer (Elementar Analysen systeme GmbH, Langensfeld, Germany).

Single-Crystal X-ray diffraction

The single-crystals X-ray diffraction data for $(2-2H)_23_2Co_6$ were collected at 173(2) K on a Bruker Apex-II-CCD diffractometer equipped with an Oxford Cryosystem liquid N_2 device, using graphite-monochromated $Mo-K\alpha$ ($\lambda = 0.71073 \text{ \AA}$) radiation. For all structures, diffraction data were corrected for absorption. Structures were solved using SHELXS-97 and refined by full matrix least-squares on F^2 using SHELXL-97. Hydrogen atoms were introduced at calculated positions and refined using a riding model.⁵⁹

The single-crystals X-ray diffraction data for $(2-2H)_23_2Ni_6$ were collected on the 'Belok' beamline of Kurchatov Synchrotron Radiation Source (National Research Center 'Kurchatov Institute', Moscow, Russian Federation) using a Rayonix SX165 CCD detector at $\lambda = 0.793127 \text{ \AA}$. The frames were collected using an oscillation range of 1.0° and ϕ scan mode. The data were indexed and integrated using the utility iMOSFLM from the CCP4 program suite⁶⁰ and then scaled and corrected for absorption using the Scala program.⁶¹ Structures were solved using Olex2 software⁵⁵ by direct methods with SHELXT⁶² refined by the full-matrix least-squares on F^2 using SHELXL.⁵⁹ Non-hydrogen atoms were refined anisotropically.

The crystallographic data are available for free of charge downloading from the Cambridge Crystallographic Data Centre via www.ccdc.cam.ac.uk/datarequest/cif. CCDC: $(2-2H)_23_2Co_6$: 2044262 and $(2-2H)_23_2Ni_6$: 2044261.

X-ray diffraction on powder

The main text of the article should appear here with headings as appropriate. Powder diffraction studies (PXRD) diagrams were collected on polycrystalline samples at the room temperature (293(2) K), on a Bruker D8 diffractometer using monochromatic $Cu-K\alpha$ radiation with a scanning range between 2° and 40° at a scan step size of 2° min^{-1} .

The time depended PXDR patterns were recorded in the 2θ range between 2 and 40° , in 0.016° steps, with a step time of 0.1 (for freshly prepared sample) and 0.5 s (for consecutive scans of the air-dried sample) upon the sample holder rotating at 15 rpm.

The PXRD patterns for samples studied by DVS method were measured on a Bruker D8 ADVANCE ECO diffractometer equipped with Cu K α radiation source in the Debye-Scherrer geometry. The samples were stabilised to constant mass under controlled temperature and humidity conditions in glass capillaries and subsequently sealed.

TGA measurements

Thermal stability was studied using a STA 449C Jupiter synchronous microthermoanalyzer (Netzsch, Germany) at heating rate of 10 $^\circ$ /min under argon atmosphere.

N₂ adsorption properties

Nitrogen adsorption-desorption isotherms were determined by the standard method at 77 K using an Autosorb iQ (Quantachrome) static volumetric apparatus. Before adsorption the samples were outgassed at 50 $^\circ$ C overnight using turbomolecular pump to remove adsorbed water.

Dynamic vapor sorption studies

The solvent vapor sorption isotherms were measured at 298 K with a Dynamic Vapor Sorption method using an SMS DVS Resolution apparatus in the p/p_0 range from 0 to 98% (H₂O), 95% (MeOH), 90% (EtOH) or 80% (CH₃C(O)CH₃) in N₂ carrier gas. The samples were initially activated by exposure to 30% RH at 323 K followed by dehydration at 323 K and 0% RH. All activation and measurement steps were carried out to achieve stable mass of the samples ($dm/dt = \pm 0.002\%$ min⁻¹).

SEM microscopy

Autosorb iQ SEM images were obtained using HITACHI S-4700 scanning electron microscope at the accelerating voltage of 20 kV.

Conclusions

The formation of metallacyclic hexameric moieties results from the self-assembly process involving (2-4H) and the highly coordinating (3-4H) macrocyclic ligands, together with divalent metallic cations. Whereas when a metallic cation and (3-4H), are combined with an analogous calixarene species presenting a longer propylene spacer (4-4H), only a trinuclear species is obtained,⁵² when using a shorter methylene spacer, the formation of symmetrical hexanuclear coordination compounds of general formula ((2-2H)₂3₂M₆, M = Co, Ni) is observed. Its structure is arising from a reproducible stepwise formation in solution of the [3(M₃DMF(OH₂)₂)²⁺ entities, that are then connected with by (2-4H)²⁻ species. The resulting molecular compound adopts a ring shape with a round cavity, which forms internal channels in the crystalline structure. Some H₂O and DMF molecules are also present in the coordination sphere of the metallic cations. In the crystals, the packing of the

hexameric units leads also to the formation of external channels. Irreversible structural transformation of both compounds was observed upon exposure to air, that reveal to be stable through desolvation (release of lattice solvent molecules). In addition, an interesting phenomenon of reversible and reproducible humidity-assisted desorption of lattice DMF was observed.

Due to intrinsic porosity and also to the presence of robust internal channels, the guest binding behavior for prepared microcrystalline coordination complexes was investigated at the solid gaseous interface, demonstrating good sorption ability towards water, acetone and lower alcohol molecules (methanol and ethanol). Both (2-2H)₂3₂Ni₆ and (2-2H)₂3₂Co₆ show a marked preference for the sorption of organic solvents displaying much stronger polarizability than smaller and "harder" water molecules. This trend can be expected and does fairly match with that found in the previously reported works showing a high hydrophobic character and sorption capacity of calix[4]arene backbones.⁴⁴⁻⁴⁷

This impact into the chemistry of calix[4]arene based coordination compounds, with controlled nuclearities and shape, represents an important step towards further development of macrocyclic based complexes, and their uses; for example, the new upper rim calix[4]arene dicarboxylates may afford similar types of supramolecular architectures, but with tunable pore sizes. These studies are in progress, also with a view to fine-tuning the cluster cores in order to achieve greater control over sorption properties and self-assembly pattern of such supramolecular systems.

Author Contributions

The manuscript was written through contributions of all authors. All authors have given approval to the final version of the manuscript.

Conflicts of interest

There are no conflicts to declare.

Acknowledgements

This work was supported by Russian Science Foundation (project № 19-73-20035). The authors are grateful to Kurchatov Institute for performing of XRD-analysis, to Spectral-Analytical Center of FRC Kazan Scientific Center of RAS for their help and support in TGA, PXRD and IR studies. A.G., A.S. S.K. and E.P. acknowledge the support by the Government assignment for FRC Kazan Scientific Center of RAS. Financial support from the University of Strasbourg, the Institut Universitaire de France and the CNRS are also acknowledged. The authors thank Ms. Gabriela Jajko and Prof. Wacław Makowski for N₂ adsorption measurements.

Notes and reference

- 1 A.M.P. Peedikakkal, N.N. Adarsh, 2019 Porous Coordination Polymers. In: Jafar Mazumder M., Sheardown H., Al-Ahmed A. (eds) Functional Polymers. Polymers and Polymeric Composites: A Reference Series. Springer, Cham. https://doi.org/10.1007/978-3-319-92067-2_5-1
- 2 E.-S.M. El-Sayed, D. Yuan Metal-Organic Cages (MOCs): From Discrete to Cage-based Extended Architectures. *Chem. Lett.* 2020, **49**, 2853.
- 3 E.J. Gosselin, C.A. Rowland, E.D. Bloch Permanently Microporous Metal-Organic Polyhedra. *Chem. Rev.* 2020, **120**, 16, 8987-9014.
- 4 N. Lia, R. Feng, J. Zhu, Z. Chang, X.-H. Bu, Conformation versatility of ligands in coordination polymers: From structural diversity to properties and applications, *Coord. Chem. Rev.*, 2018, **375**, 558-586.
- 5 H.-Y. Li, S.-N. Zhao, S.-Q. Zang, J. Li, Functional metal-organic frameworks as effective sensors of gases and volatile compounds, *Chem. Soc. Rev.*, 2020, **49**, 6364-6401.
- 6 X. Zhang, W. Wang, Z. Hu, G. Wang, K. Uvdal, Coordination polymers for energy transfer: Preparations, properties, sensing applications and perspectives, *Coord. Chem. Rev.*, 2015, **284**, 206-235.
- 7 J.-S. M. Lee, K.-I. Otake, S. Kitagawa, Transport properties in porous coordination polymers, *Coordination Chemistry Reviews*, 2020, **421**, 213447.
- 8 A. G. Slater, A. I. Cooper, Function-led design of new porous materials, *Science*, 2015, **348**, aaa8075.
- 9 M. A. Little, A. I. Cooper, The Chemistry of Porous Organic Molecular Materials, *Adv. Funct. Mater.* 2020, **30**, 1909842.
- 10 S. Tashiro, M. Shionoya, Novel Porous Crystals with Macrocyclic-Based Well-Defined Molecular Recognition Sites, *Acc. Chem. Res.*, 2020, **53**, 632-643.
- 11 C. D. Gutsche, in *Calixarenes Revised: Monographs in Supramolecular Chemistry* Vol. **6**, The Royal Society of Chemistry, Cambridge, 1998.
- 12 A. Ikeda, S. Shinkai, Novel Cavity Design Using Calix[n]arene Skeletons: Toward Molecular Recognition and Metal Binding *Chem. Rev.*, 1997, **97**, 1713-1734.
- 13 N. Morohashi, T. Hattori, Selective guest inclusion by crystals of calixarenes: potential for application as separation materials, *J Incl Phenom Macrocycl Chem*, 2018, **90**, 261-277.
- 14 A. Ovsyannikov, S. Solovieva, I. Antipin, S. Ferlay Coordination Polymers based on calixarene derivatives: Structures and properties. *Coord. Chem. Rev.* 2017, **352**, 151-186.
- 15 H. Kumagai, M. Hasegawa, S. Miyanari, Y. Sugawa, Y. Sato, T. Hori, S. Ueda, H. Kamiyama, S. Miyano, Facile synthesis of p-tert-butylthiacalix[4]arene by the reaction of p-tert-butylphenol with elemental sulfur in the presence of a base, *Tetrahedron Lett.*, 1997, **38**, 3971-3972.
- 16 B.S. Creavena, D.F. Donlona, J. McGinley Coordination chemistry of calix[4]arene derivatives with lower rim functionalisation and their applications *Coord. Chem. Rev.* 2009, **253**, 893-962.
- 17 G. Karotsis, S. J. Teat, W. Wernsdorfer, S. Piligkos, S. J. Dalgarno, E. K. Brechin, Calix[4]arene-Based Single-Molecule Magnets *Angew. Chem. Int. Ed.* 2009, **48**, 8285-8288.
- 18 S. M. Taylor, G. Karotsis, R. D. McIntosh, S. Kennedy, S. J. Teat, C. M. Beavers, W. Wernsdorfer, S. Piligkos, S. J. Dalgarno, E. K. Brechin, A Family of Calix[4]arene-Supported [Mn^{III}₂Mn^{II}]₂ Clusters *Chem. Eur. J.* 2011, **17**, 7521-7530.
- 19 T. Kajiwara, N. Iki, M. Yamashita, Transition metal and lanthanide cluster complexes constructed with thiacalix[n]arene and its derivatives *Coord. Chem. Rev.*, 2007, **251**, 1734-1746.
- 20 G. Mislin, E. Graf, M. W. Hosseini, A. De Cian, Sulfone-calixarenes: a new class of molecular building block *J. Chem. Soc. Chem. Commun*, 1998, 1345-1346.
- 21 N. Iki, H. Kumagai, N. Morohashi, K. Ejima, M. Hasegawa, S. Miyanari, S. Miyano, Selective oxidation of thiacalix[4]arenes to the sulfinyl- and sulfonylcalix[4]arenes and their coordination ability to metal ions. *Tetrahedron Lett.* 1998, **39**, 7559-7562.
- 22 T. Kajiwara, T. Kobashi, R. Shinagawa, T. Ito, S. Takaishi, M. Yamashita, N. Iki, Highly Symmetrical Tetranuclear Cluster Complexes Supported by p-tert-Butylsulfonylcalix[4]arene as a Cluster-Forming Ligand *Eur. J. Inorg. Chem.* 2006, 1765-1770.
- 23 F.-R. Dai, U. Sambasivam, A. J. Hammerstrom, Z. Wang, Synthetic Supercontainers Exhibit Distinct Solution versus Solid State Guest-Binding Behavior *J. Am. Chem. Soc.* 2014, **136**, 7480-7491.
- 24 N. L. Netzer, F.-R. Dai, Z. Wang, C. Jiang pH-Modulated Molecular Assemblies and Surface Properties of Metal-Organic Supercontainers at the Air-Water Interface *Angew. Chem. Int. Ed.* 2014, **53**, 10965-10969.
- 25 M. Liu, W. Liao, C. Hu, S. Du, H. Zhang, Calixarene-Based Nanoscale Coordination Cages *Angew. Chem. Int. Ed.* 2012, **51**, 1585-1588.
- 26 K. Xiong, F. Jiang, Y. Gai, D. Yuan, L. Chen, M. Wu, K. Su, M. Hong, Truncated octahedral coordination cage incorporating six tetranuclear-metalbuilding blocks and twelve linear edges *Chem. Sci.*, 2012, **1**, 2321-2325.
- 27 Y. Bi, S. Du, W. Liao, Thiacalixarene-based nanoscale polyhedral coordination cages *Coord. Chem. Rev.*, 2014, **276**, 61-72.
- 28 X. Hang, B. Liu, X. Zhu, S. Wang, H. Han, W. Liao, Y. Liu, C. Hu, Discrete {Ni₄₀} Coordination Cage: A Calixarene-Based Johnson-Type (J17) Hexadecahedron. *J. Am. Chem. Soc.* 2016, **138**, 2969-2972.
- 29 D. Geng, L. Huang, X. Han, Y. Bi, Y. Qin, Q. Li, K. Zhou, L. Song, Z. Zheng, Merohedral icosahedral M₄₈ (M 1/4 Co^{II}, Ni^{II}) cage clusters supported by thiacalix[4]arene *Chem. Sci.*, 2018, **9**, 8535-8541.
- 30 K. Zhang, S.-W. Du, A novel series of giant cobalt-calixarene macrocycles: ring-expansion and modulation of pore apertures through recrystallization *Dalton Trans.*, 2021, **50**, 6181-6187.
- 31 N. Bhuvanewari, F.-R. Dai, Z.-N. Chen, Sensitive and Specific Guest Recognition through Pyridinium- Modification in Spindle-Like Coordination Containers *Chem. Eur. J.* 2018, **24**, 6580-6585.
- 32 C.-Z. Sun, L.-J. Cheng, Y. Qiao, L.-Y. Zhang, Z.-N. Chen, F.-R. Dai, W. Lin, Z. Wang, Stimuli-responsive metal-organic supercontainers as synthetic proton receptors *Dalton Trans.*, 2018, **47**, 10256-10263.
- 33 Y. Fang, Z. Xiao, J. Li, C. Lollar, L. Liu, X. Lian, S. Yuan, S. Banerjee, P. Zhang, H.-C. Zhou, Formation of a Highly Reactive Cobalt Nanocluster Crystal within a Highly Negatively Charged Porous Coordination Cage *Angew. Chem. Int. Ed.* 2018, **57**, 5283-5287.
- 34 Y. Qiao, L. Zhang, J. Li, W. Lin, Z. Wang, Switching on Supramolecular Catalysis via Cavity Mediation and Electrostatic Regulation *Angew. Chem. Int. Ed.* 2016, **55**, 12778-12782.
- 35 C. Tan, J. Jiao, Z. Li, Y. Liu, X. Han, Y. Cui, Design and Assembly of a Chiral Metallosalen-Based Octahedral Coordination Cage for Supramolecular Asymmetric Catalysis, *Angew. Chem. Int. Ed.* 2018, **57**, 2085-2090.

- 36 S. Wang, X. Gao, X. Hang, X. Zhu, H. Han, W. Liao, W. Che Ultrafine Pt Nanoclusters Confined in a Calixarene-Based {Ni₁₂} Coordination Cage for High-Efficient Hydrogen Evolution Reaction *J. Am. Chem. Soc.* 2016, **138**, 16236-16239.
- 37 M. M. Deegan, T. S. Ahmed, G. P. A. Yap, E. D. Bloch, Structure and redox tuning of gas adsorption properties in calixarene-supported Fe(II)-based porous cages *Chem. Sci.*, 2020, **11**, 5273-5279.
- 38 J. L. Atwood, L. J. Barbour, A. Jerga, Storage of Methane and Freon by Interstitial van der Waals Confinement *Science* 2002, **296**, 2367-2369
- 39 J. L. Atwood, L. J. Barbour, A. Jerga, B. L. Schottel, Guest Transport in a Nonporous Organic Solid via Dynamic van der Waals Cooperativity *Science* 2002, **298**, 1000-1002.
- 40 P. K. Thallapally, S. J. Dalgarno, J. L. Atwood, Frustrated Organic Solids Display Unexpected Gas Sorption *J. Am. Chem. Soc.* 2006, **128**, 15060-15061.
- 41 P. K. Thallapally, L. Dobrzanska, T. R. Gingrich, T. B. Wirsig, L. J. Barbour, J. L. Atwood, Acetylene Adsorption and Binding in a Nonporous Crystal Lattice *Angew. Chem. Int. Ed.* 2006, **45**, 6506-6509.
- 42 G. S. Ananchenko, I. L. Moudrakovski, A. W. Coleman, J. A. A. Ripmeester, Channel-Free Soft-Walled Capsular Calixarene Solid for Gas Adsorption *Angew. Chem. Int. Ed.* 2008, **47**, 5616-5618.
- 43 M. A. Sinnwell, J. L. Atwood, P. K. Thallapally, Sorption of CO₂ in a hydrogen-bonded diamondoid network of sulfonylcalix[4]arene, *Supramolecular chemistry*, 2018, **30**, 540-544.
- 44 M. A. Ziganshin, L. R. Validova, I. S. Antipin, I. I. Stoikov, A. I. Konovalov, V. V. Gorbachuk, Structure-property relationship for clathrates formed in systems with guest vapor and 1,3-disubstituted tert-butylcalix[4]arene. *Journal of Structural Chemistry*, 2005, **46**, S33-S38.
- 45 V. V. Gorbachuk, L. S. Savelyeva, M. A. Ziganshin, I. S. Antipin, V. A. Sidorov, Molecular recognition of organic guest vapor by solid adamantylcalix[4]arene *Russ. Chem. Bull., Int. Ed.*, 2004, **53**, 60-65.
- 46 G. D. Safina, M. A. Ziganshin, I. I. Stoikov, I. S. Antipin, V. V. Gorbachuk, Configuration effect of the tertbutylthiacalix[4]arene tetracarboxy derivative on its receptor properties toward vaporous organic compounds, *Russian Chemical Bulletin*, 2009, **58**, 71-79.
- 47 N. Morohashi, K. Ebata, H. Nakayama, S. Noji, T. Hattori, Competitive Inclusion of Carboxylic Acids with a Metastable Crystal Polymorph of p-tert-Butylthiacalix[4]arene, *Cryst. Growth Des.* 2017, **17**, 891-900.
- 48 X. Hang, B. Liu, S. Wang, Y. Liu, W. Liao, A metal-calixarene coordination nanotube with 5-(pyrimidin-5-yl)isophthalic acid. *Dalton Trans.* 2018, **47**, 1782-1785.
- 49 Z. Zhang, A. Drapailo, Y. Matvieiev, L. Wojtas, M. J. Zaworotko, A calixarene based metal organic material, calixMOM, that binds potassium cations *Chem. Commun.*, 2013, **49**, 8353-8355.
- 50 Y. Ishii, Y. Takenaka, K. Konishi, Porous Organic-Inorganic Assemblies Constructed from Keggin Polyoxometalate Anions and Calix[4]arene-Na⁺ Complexes: Structures and Guest-Sorption Profiles. *Angew. Chem. Int. Ed.* 2004, **43**, 2702-2705.
- 51 P. Murphy, S. J. Dalgarno, M. J. Paterson, Transition Metal Complexes of Calix[4]arene: Theoretical Investigations into Small Guest Binding within the Host Cavity. *J. Phys. Chem. A* 2016, **120**, 5, 824-839.
- 52 M. V. Kniazeva, A. S. Ovsyannikov, D. R. Islamov, A. I. Samigullina, A. T. Gubaidullin, S. E. Solovieva, I. S. Antipin, S. Ferlay, Formation of Unsymmetrical Trinuclear Metallamacrocycles Based on Two Different Cone Calix[4]arene Macrocyclic Rings. *Crystals* 2020, **10**, 364.
- 53 M. V. Kniazeva, A. S. Ovsyannikov, D. R. Islamov, A. I. Samigullina, A. T. Gubaidullin, P. V. Dorovatovskii, S. E. Solovieva, I. S. Antipin, S. Ferlay, Nuclearity control in calix[4]arene based zinc (II) coordination complexes. *CrystEngComm* 2020, **22**, 7693-7703.
- 54 A. L. Spek, Single-crystal structure validation with the program PLATON *J. Appl. Crystallogr.*, 2003, **36**, 7-13.
- 55 O. V. Dolomanov, L. J. Bourhis, R. J. Gildea, J. A. Howard, H. Puschmann, OLEX2: a complete structure solution, refinement and analysis program. *J. Appl. Cryst.*, 2009, **42**, 339-341.
- 56 A. J. Fletcher, E. J. Cussen, D. Bradshaw, M. J. Rosseinsky, K. M. Thomas, Adsorption of Gases and Vapors on Nanoporous Ni₂(4,4'-Bipyridine)₃(NO₃)₄ Metal-Organic Framework Materials Templated with Methanol and Ethanol: Structural Effects in Adsorption Kinetics *J. Am. Chem. Soc.* 2004, **126**, 9750-9759.
- 57 I. Akhmetova, S. Beyer, K. Schutjajew, T. Tichter, M. Wilke, C. Prinz, I. C. B. Martins, D. Al-Sabbagh, C. Roth, F. Emmerling, Cadmium benzylphosphonates – the close relationship between structure and properties *CrystEngComm*, 2019, **21**, 5958-5964.
- 58 E. M. Collins, M. A. McKervey, E. Madigan, M. B. Moran, M. Owens, G. Ferguson, S. J. Harris, Chemically Modified Calix[4]arenes. Regioselective Synthesis of 1,3-(Distal) Derivatives and Related Compounds. X-Ray Crystal Structure of a Diphenol- Dinitrile, *J. Chem. Soc. Perkin Trans. 1*, 1991, 3137-3142.
- 59 G. M. Sheldrick, A short history of SHELX *Acta Crystallogr.* 2008, **A64**, 112-122.
- 60 T.G. Batty, L. Kontogiannis, O. H. Johnson, R. Powell, A.W. Leslie, iMOSFLM: a new graphical interface for diffraction-image processing with MOSFLM. *Acta Cryst.*, 2011, **D67**, 271-281.
- 61 P.R. Evans, Scaling and assessment of data quality. *Acta Cryst.*, 2006, **D62**, 72-82.
- 62 G. M. Sheldrick, SHELXT: Integrating space group determination and structure solution. *Acta Cryst.*, 2015, **A71**, 3-8.

	(2-2H)₂3Co₆	(2-2H)₂3Ni₆
Formula	C ₁₈₂ H ₂₂₄ Co ₆ N ₂ O ₄₆ S ₈ , 10(C ₃ H ₇ NO)[+ solvent]	C ₁₈₂ H ₂₁₈ Ni ₆ N ₂ O ₄₆ S ₈ , 4(C ₃ H ₇ NO)[+ solvent]
Molecular weight (gmol ⁻¹)	4516.63	4070.69
Crystal system	triclinic	triclinic
Space group	P-1	P-1
a(Å)	12.8987(5)	12.807(3)
b(Å)	21.7263(7)	21.556(4)
c(Å)	24.4931(9)	24.370(5)
α(deg)	103.796(2)	104.15(3)
β(deg)	91.187(2)	91.44(3)
γ(deg)	104.747(2)	104.95(3)
V(Å ³)	6422.1(4)	6275(2)
Z	1	1
Colour	Light rose	Light green
Crystal dim (mm ³)	0.100 x 0.120 x 0.120	0.060 x 0.050 x 0.040
Dcalc (gcm ⁻³)	1.168	1.077
F(000)	2388	2148
μ (mm ⁻¹)	0.514	0.779
Wavelength (Å)	0.71073	0.793127
Temperature (K)	173	100
Number of data meas.	27931	23793
Number of data with I > 2σ(I)	20786	12766
R (%)	0.1058	0.088
Rw (%)	0.1325	0.1370
GOF	1.576	0.985
Largest peak in final difference (eÅ ⁻³)	1.964	1.786

Table 1: Crystallographic Parameters for **(2-2H)₂3Co₆** and **(2-2H)₂3Ni₆**.